

Dynamic Monte Carlo Simulation of the NO + CO Reaction on Rh(111)

L. A. Avalos,[†] V. Bustos,[‡] R. Uñac,[‡] F. Zaera,[§] and G. Zgrablich^{*,‡}

Departamento de Química, Universidad Autónoma Metropolitana, Iztapalapa, México, Laboratorio de Ciencias de Superficies y Medios Porosos, Universidad Nacional de San Luis, 5700 San Luis, Argentina, and Department of Chemistry, University of California, Riverside, California 92521

Received: August 2, 2006; In Final Form: October 9, 2006

The kinetics of the catalytic reduction of NO by CO on Rh(111) surfaces was investigated by using dynamic Monte Carlo simulations. Our model takes into account recent experimental findings and introduces relevant modifications to the classical reaction scheme, including an alternative pathway to produce N₂ through an (N–NO)* intermediate, the formation of atomic nitrogen islands in the adsorbed phase, and the influence of coadsorbed species on the dissociation of NO. All elementary steps are expressed as activated processes with temperature-dependent rates and realistic values dictated by experiments. Calculated steady-state phase diagrams are presented for the NO + CO reaction showing the windows for the conditions under which the reaction is viable. The model predicts variations in both production rates and adsorbate coverages with temperature consistent with experimental data. The effect of varying the individual kinetic parameters and the importance of each step in the reaction scheme were probed.

1. Introduction

The catalytic reduction of NO by CO (and other reducing agents) promoted by transition metals has received a great deal of attention in connection with its relevance to problems of pollution control in the atmosphere.^{1–3} To date, rhodium has proven to be the best catalyst for this reduction.⁴ Extensive experimental investigations using model surfaces have also shown that Rh(111), the expected predominant facet in metal nanoclusters dispersed on catalyst supports, is especially adept for the promotion of this reaction.^{5–12} Consequently, much theoretical modeling has been performed to attempt to understand its kinetics.^{13–18} In spite of the extensive past work in this area, however, renewed interest has emerged in the past few years because of new molecular-level information about the reaction mechanism derived from new experimental and theoretical reports.

Indeed, our recent molecular beam experiments on the reduction of NO over Rh(111)^{8,19–26} have indicated that the standard reaction scheme used to explain the kinetics of the reaction needs to be modified in at least two important ways. The first stems from the observation that when a ¹⁴N-covered Rh(111) surface is exposed to a ¹⁵NO + CO beam, the molecular nitrogen produced always contains at least one ¹⁵N atom.^{21,22,25} This means that the recombination of nitrogen atoms on the surface, usually assumed to be the step responsible for the formation of molecular nitrogen, is in fact not fast enough under typical reaction conditions to account for such N₂ production. Instead, an intermediate species, (N–NO)*, appears to form on the surface and then decomposes to N₂(gas) + O(ads). Therefore, in a realistic description of the overall NO + CO reaction, both the atomic recombination of nitrogen atoms and the formation of this (N–NO)* intermediate should be considered in parallel, with the latter being the dominant one. To this

it should be added that the formation of the (N–NO)* species may be enhanced by the presence of coadsorbed NO molecules.²⁵

A second important modification to the NO reduction mechanism brought about by the molecular beam work stems from the evidence that, at least on Rh(111), the atomic nitrogen produced by NO decomposition forms compact islands on the rhodium surface.^{19,20,22} Indeed, it was found that the isotopic distribution of the molecular nitrogen detected in temperature programmed desorption (TPD) spectra from surfaces prepared by using isotopic mixtures of ¹⁴N- and ¹⁵N-labeled nitrogen oxide can only be explained on that basis.^{22,24} The mechanism for the formation of these islands has not yet been established. As can be easily imagined, both modifications in the molecular mechanism are expected to lead to important changes in the behavior of the kinetics of the reaction.

Theoretical studies on the kinetics of the NO + CO surface reaction have so far focused mainly on establishing the precise conditions under which a reactive state can be sustained, that is, on calculating steady-state phase diagrams and characterizing the window of parameters under which the reaction operates. This window is usually limited by two kinetic phase transitions, so much emphasis has been placed on identifying how such a phase diagram is affected by different assumptions in the molecular mechanism.^{13–18,27–33} In view of the complexity of the reaction, lattice-gas models and Monte Carlo simulations have been the main techniques used for these studies. The theoretical work has followed the evolution of experimental findings and has evolved from early studies based on classical reaction schemes^{13–16,18,27–29} to more recent calculations that progressively incorporate new molecular-beam experimental findings.^{17,30–33}

In our studies of the particular case of the reduction of NO on Rh(111), the first effect studied was the introduction of the formation of an (N–NO)* intermediate as the principal step for the production of N₂.³⁰ Although new physical insight for the process was gained, no satisfactory agreement with experi-

* Corresponding author. E-mail: giorgio@unsl.edu.ar.

[†] Universidad Autónoma Metropolitana.

[‡] Universidad Nacional de San Luis.

[§] University of California.

mental observations was obtained in terms of the calculated phase diagrams and coverage evolution of the different species. In particular, the predicted high coverage of atomic oxygen on the surface at low gas-phase CO pressures was in total contradiction with experiments. This provided a strong indication that NO dissociation must be depressed by the presence of other coadsorbed NO species, as in fact had been shown directly by Niemantsverdriet and co-workers.³⁴ A new model incorporating both this NO dissociation inhibition effect and a process to allow for N island formation predicted a behavior in substantially better agreement with experimental observations,³² even though it completely neglected the nitrogen recombination step.

A more realistic model taking into account all of the experimental evidence, namely, the production of N₂ through two parallel processes, N recombination and (N–NO)* formation (the latter being dominant), the formation of N islands, and the inhibition of NO dissociation by the presence of neighboring coadsorbed NO, produced encouraging results.³³ Nevertheless, even that model should be considered as tentative, since all elementary processes were assigned arbitrary and fixed reaction rates and were considered not to depend on temperature. The description of the kinetic evolution of the system by using appropriate temperature-dependent rates for each of the elementary steps involved is the purpose of the present work. This is done by using dynamic Monte Carlo simulations with a time evolution determined by using reported values for the rates of the elementary processes.

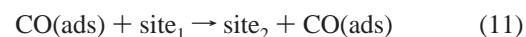
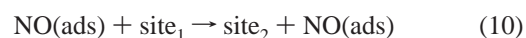
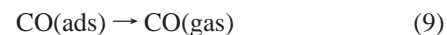
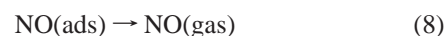
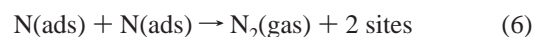
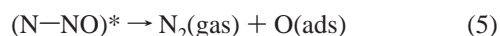
In Section 2 we describe the lattice-gas model, the reaction scheme, and the simulation method used to follow the kinetics of the system. The results of these simulations are presented, discussed, and compared with experimental data in Section 3, and our conclusions are given in Section 4.

2. Model and Simulation Method

In our lattice-gas model the surface of a Rh(111) single crystal is represented as a triangular lattice of $L \times L$ adsorption sites with periodic boundary conditions. The gas phase is assumed to be a mixture of NO and CO molecules with molar fractions Y_{NO} and Y_{CO} , respectively, adding up to a total value of 1. Our reaction scheme takes into account the following:

- (a) the formation of an (N–NO)* intermediate as the principal step for the production of N₂,
- (b) an alternative production of N₂ via the classical N recombination step,
- (c) the formation of N islands on the surface,
- (d) the inhibition of the dissociation of NO due to the presence of neighboring adsorbed particles,
- (e) the desorption of NO and CO species, and
- (f) the surface diffusion of NO and CO species.

The proposed reaction scheme can be written as follows:



As it can be observed, in this reaction scheme N₂ is produced through two parallel pathways, the conventional N + N recombination step (step 6), and an alternative path involving the formation of an (N–NO)* intermediate species (steps 4 and 5). From these, the former was made the slower of the two by choosing appropriate rate parameters. Both the inhibition of NO dissociation by coadsorbates and the formation of N islands are also taken into account by defining appropriate NO dissociation rates, as indicated below. The diffusion of adsorbed NO and CO species is represented in steps 10 and 11.

In order to operate with a relatively simple and manageable reaction scheme, we have incorporated the following additional assumptions in devising our surface reaction mechanism:

(i) The production of gas-phase N₂O is not taken into account. The rate of N₂O desorption is expected to be low compared to its decomposition on the surface via step 5, at least under low-pressure conditions.²⁶

(ii) Lateral interactions among different ad-species suggested by experimental studies^{35–39} are not considered here in the usual way, but rather in an indirect way due to the following reasons. (a) One of the most important of these interactions should be the one acting between N atoms, leading to the formation of N-islands. However, preliminary simulations showed that it was not possible to find a combination of N–N interactions which would produce N-islands with the same properties as those observed experimentally. Therefore we rather assume a kinetic mechanism for the formation of these islands, that is, NO dissociation is favored in the presence of adsorbed N atoms. (b) The experimentally observed³⁴ inhibition effect of coadsorbed NO species on the dissociation of NO cannot be easily taken into account by usual lateral interactions and, again, it will be taken into account by properly modifying the NO dissociation rate.

(iii) Oxygen desorption is neglected, since experiments have shown that this process occurs at temperatures above 600 K.^{26,40–42} In our simulations, NO reduction is only considered from 450 to 550 K.

(iv) The diffusion of oxygen atoms is not included, as this process is expected to be slower than the remaining reaction steps because of their strong bonding to the surface.

(v) N diffusion is neglected as well, also because it is likely to be slow.^{24,25,43,44} It should be noted, though, that since NO diffusion is considered in these simulations, N and NO species can still easily meet at two nearest-neighbor (nn) cells. This is important in view of the fact that in our reaction scheme N₂ is produced preferentially through the formation of an (N–NO)* intermediate, in contrast with the classical reaction scheme where N₂ is only formed through the recombination of two adsorbed N atoms.

Our system undergoes a diffusion-reaction process which cannot be treated through mean field kinetics equations, due to the fact that density fluctuations play a fundamental role in our model.⁴⁵ In fact, the presence of just one NO coadsorbed species

TABLE 1: Values of the Kinetic Parameters Used in the Monte Carlo Simulations Reported Here^a

elementary step	pre-exponential factor, ν (s^{-1})	activation energy, E (kcal mol^{-1})
NO desorption	0.1×10^{11}	26.0
CO desorption	0.1×10^{13}	31.0
NO diffusion	0.2×10^4	8.0
CO diffusion	0.2×10^4	8.0
NO dissociation	1.9×10^8	20.5
$\text{NO} + \text{N} \rightarrow \text{N}_2 + \text{O}$	1.0×10^8	21.0
$\text{N} + \text{N} \rightarrow \text{N}_2$	2.3×10^{10}	27.0
$\text{CO} + \text{O} \rightarrow \text{CO}_2$	3.5×10^6	16.0

^a Initial sticking coefficients, S_0 : NO = 0.3, CO = 0.2. Pressure in the gas phase, $p = 0.33 \times 10^{-6}$ Torr.

modifies strongly the dissociation rate of a neighboring NO. Therefore, dynamic Monte Carlo simulations must be used, based on the assumption that the time evolution of the system occurs as a Markovian stochastic process, where the time evolution of the probability distribution of the states of the physical systems is described by the master equation:⁴⁶

$$\frac{\partial P_\alpha(t)}{\partial t} = \sum_\beta [W_{\beta \rightarrow \alpha} P_\beta(t) - W_{\alpha \rightarrow \beta} P_\alpha(t)] \quad (12)$$

Here, $P_\alpha(t)$ and $P_\beta(t)$ are the probabilities to find the system in given configurations α and β , respectively, at time t , and can be considered as components of a vector \mathbf{P} representing the probability distribution of the whole set of system configurations, and W is the transition probability per unit time of the process indicated in the subscript.

These simulations can be performed through the “random selection method” which, adapted to our system, goes as follows:

- (i) a surface site is selected at random with probability $1/N$;
- (ii) a given i -type reaction step (i.e., adsorption, desorption, diffusion, etc.) is chosen at random with probability W_i/R , where R is the sum of the rates of all possible processes, i.e., the total transition rate constant of the system;
- (iii) if the selected i -type reaction step is viable for the chosen site, then it is executed; and
- (iv) the time is increased by Δt according to

$$\Delta t = -\frac{\ln \xi}{R} \quad (13)$$

where ξ is a random number between 0 and 1. This equation renders the real time evolution of the reaction.

The following elementary reaction steps and their corresponding rate constants, with the parameter values given in Table 1 (taken from the literature),^{15,20,34,47} are considered.

A. Adsorption. The impinging flux of molecules of species i from the gas phase onto the surface is given by

$$J_i = \frac{Y_i p}{(2\pi m_i kT)^{1/2}} \quad (14)$$

where J_i is the flux of NO or CO molecules per m^2 and per second, Y_i is the molar fraction of the i -type molecule in the gas phase, m_i is its mass, k is the Boltzmann constant, p is the pressure in the gas phase, and T is the absolute temperature. The adsorption rate W_i of particles impinging on the surface per cell and per second is then obtained as

$$W_i = J_i A S_0 \quad (15)$$

where A is the area per site on the surface and S_0 is the initial sticking coefficient.

B. Desorption. Desorption is considered as an activated process with a rate given by

$$W_i = \nu_i \exp(-E_{ai}/kT) \quad (16)$$

where ν_i is the frequency factor and E_{ai} the activation energy for species i .

C. Diffusion. Diffusion jumps are allowed both for CO and NO species to vacant nn sites. These jumps are performed as activated processes with rates defined by formulas as in eq 16.

D. NO Dissociation. The dissociation of NO, being a complex and the most important process included here, deserves separate consideration. The following features are taken into account:

(a) NO dissociation is facilitated by the presence of nn coadsorbed N atoms, i.e., the dissociation probability increases with the presence of nn N(ads) species. This is the mechanism we assume for the formation of N islands.

(b) Dissociation is blocked by the presence of neighboring coadsorbed NO molecules.

To include both effects, the following expression was proposed:

$$W_{\text{dis}} = \nu_{\text{dis}} \exp\{-E_{\text{dis}}[1 - (C_N n_N - C_{\text{NO}} n_{\text{NO}})]/kT\} \quad (17)$$

where ν and E are the usual pre-exponential and activation energy parameters for an activated process (given in Table 1), n_N is the number of nn sites occupied by adsorbed N, n_{NO} is the number of nn coadsorbed NO molecules, and the coefficients C are the corresponding weighting factors for those effects; the latter are parameters to be adjusted to test the effects of these interactions on the total rate of reaction and to attempt to concur with experimental observations.

E. N₂ Production. This reaction step can follow two alternative pathways:

(a) via the formation of an (N–NO)* intermediate species when two nn sites are occupied by N and NO species, respectively, or

(b) by recombination of two nn adsorbed N atoms.

Both are considered activated processes here, with frequency factors and activation energies given in Table 1. As discussed above, the $\text{N} + \text{N}$ recombination step is expected to be slower than the production of (N–NO)*, by a relation of approximately 0.3:0.7;²⁵ the corresponding rate parameters were chosen to fulfill this condition. In addition, according to the same experiments, the formation probability of (N–NO)* is believed to be enhanced by the presence of coadsorbed nn NO molecules. Therefore, the activation energy for this process was modified in a way similar to that in eq 17, in this case by a $[1 - C_{\text{N–NO}} n_{\text{NO}}]$ factor.

F. CO₂ Production. This process is possible when two nn sites are occupied by CO and O species, respectively, and takes place as an activated process with a rate given by eq 16 (with the appropriate parameters, Table 1).

A simulation run starts with a completely empty surface. A Monte Carlo step (MCS) was chosen to consist of $L \times L$ trials, so, on average, every site on the lattice is visited once to execute a possible process. A lattice size of $L = 100$ was picked to make finite size effects negligible (a fact verified by independent simulations with bigger lattices). For a given value of Y_{CO} , and starting with an initial empty surface, the process was deemed to have reached steady state when the total surface coverage θ

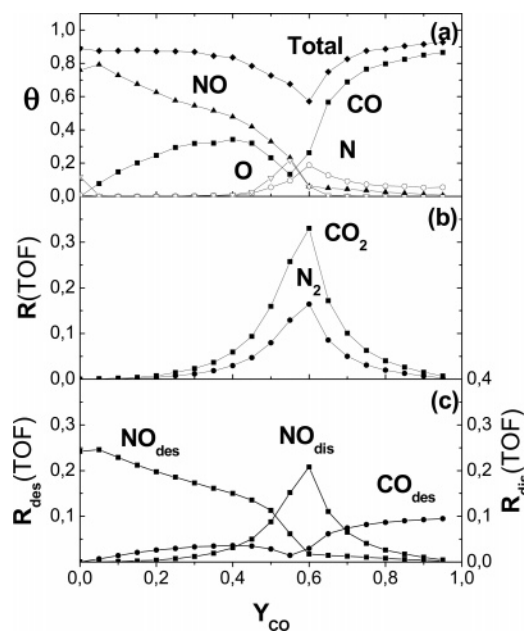


Figure 1. Steady-state coverages, θ (a), N_2 and CO_2 reaction rates, R (b), and elementary step rates, R_{des} and R_{dis} (c), as a function of CO concentration in the gas phase, Y_{CO} , obtained in our Monte Carlo simulations using the following set of parameters: $C_N = 1.0$, $C_{NO} = 0.5$, $C_{N-NO} = 0.1$, which were found to be the ones that optimally reproduce the experimental measurements on this system.

$= \theta_N + \theta_O + \theta_{NO} + \theta_{CO}$ stopped changing appreciably over the last 10^3 MCS. In all cases reported here, stabilization was achieved before 7×10^4 MCS. After the simulation was considered finished, plots of the coverage of each species and of the reaction rates R versus Y_{CO} were obtained.

3. Results and Discussion

A large number of simulations at a pressure in the gas phase $p = 0.33 \times 10^{-6}$ Torr, similar to that used in experiments, were carried out in order to understand the effect that each of the parameters involved in the model exerts on the overall kinetic behavior of the system. We begin by presenting the best results obtained when all elementary processes are active, and then we test the importance of each elementary process by turning them off one at a time.

Figure 1 shows, from top to bottom, the steady-state surface coverages of NO, CO, O, and N, the reaction rates for the production of N_2 and CO_2 , and the reaction rates for some key elementary processes (NO and CO desorption and NO dissociation), all as a function of Y_{CO} , obtained from a simulation at $T = 500$ K and with $C_N = 1.0$, $C_{NO} = 0.5$ and $C_{N-NO} = 0.1$. Similar results, not shown here, were obtained at other temperatures. With the parameters used for the calculations reported in Figure 1, the system presents a reaction window covering practically the whole range of CO molar fraction in the gas phase, that is, it reaches steady-state conditions with all gas-phase mixtures, but shows a relatively sharp reaction rate maximum at intermediate values of Y_{CO} . This coincides with the maximum rate for NO dissociation, which occurs approximately for the same gas mixture were the rates for NO desorption and CO desorption cross, stressing the importance of NO dissociation in the whole reaction. As expected, the NO coverage decreases while the CO coverage increases, except for a depression occurring around the reaction rate maximum, with increasing Y_{CO} , in the same way as the NO and CO desorption rates do. It is important to highlight here that the

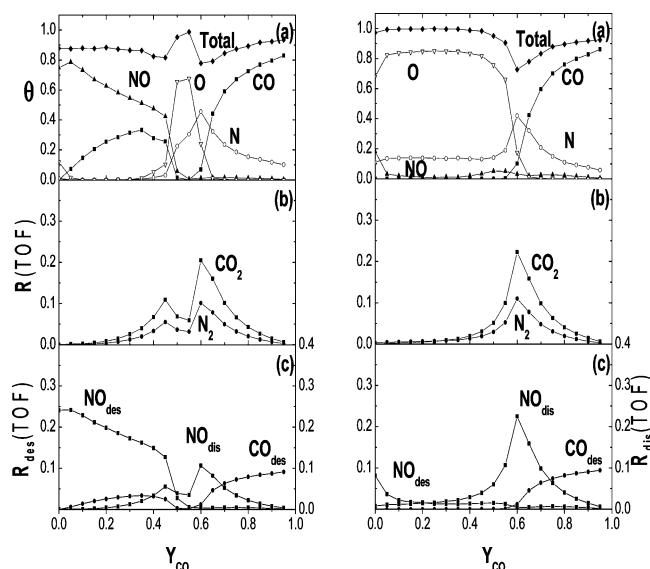


Figure 2. Left: effect of neglecting the N + N recombination step for the formation of N_2 . Right: effect of neglecting the $(N-NO)^*$ pathway for the formation of N_2 . The remaining parameters were kept the same as in Figure 1.

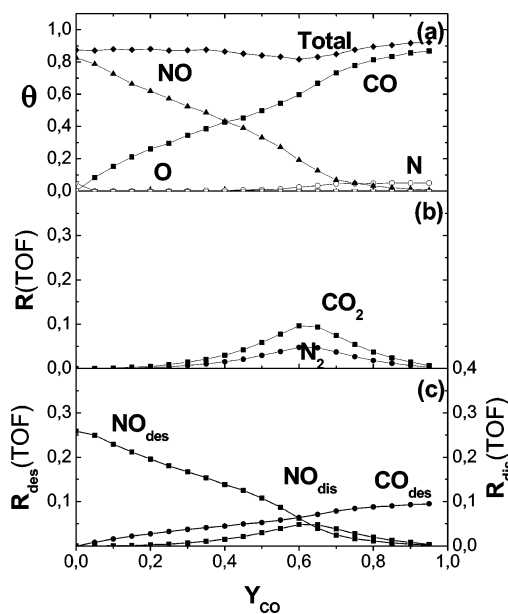


Figure 3. Effect of neglecting the process of formation of N islands by setting $C_N = 0$. The remaining parameters were kept the same as in Figure 1.

present model does not predict a high O coverage at low Y_{CO} values, a behavior definitively not observed in experiments (at least at these low temperatures) but common in many previous simulations. We also note that the O and N coverages reach significant values only around the reaction rate maximum, and they cross each other (O decreasing and N increasing) just before the maximum. This behavior also follows what has been observed experimentally.⁸

In Figure 2, left side, results are reported from simulations where the N + N recombination step (step 6 in the reaction scheme) was turned off, leaving the formation of the $(N-NO)^*$ intermediate species as the only pathway for the production of N_2 . Everything else was left the same. It can be seen there that the results are somewhat similar to those in Figure 1, at least in terms of the main trends reported: the behavior of the reaction rate is similar at high Y_{CO} values (even if it develops an additional local maximum at lower values), and the behavior

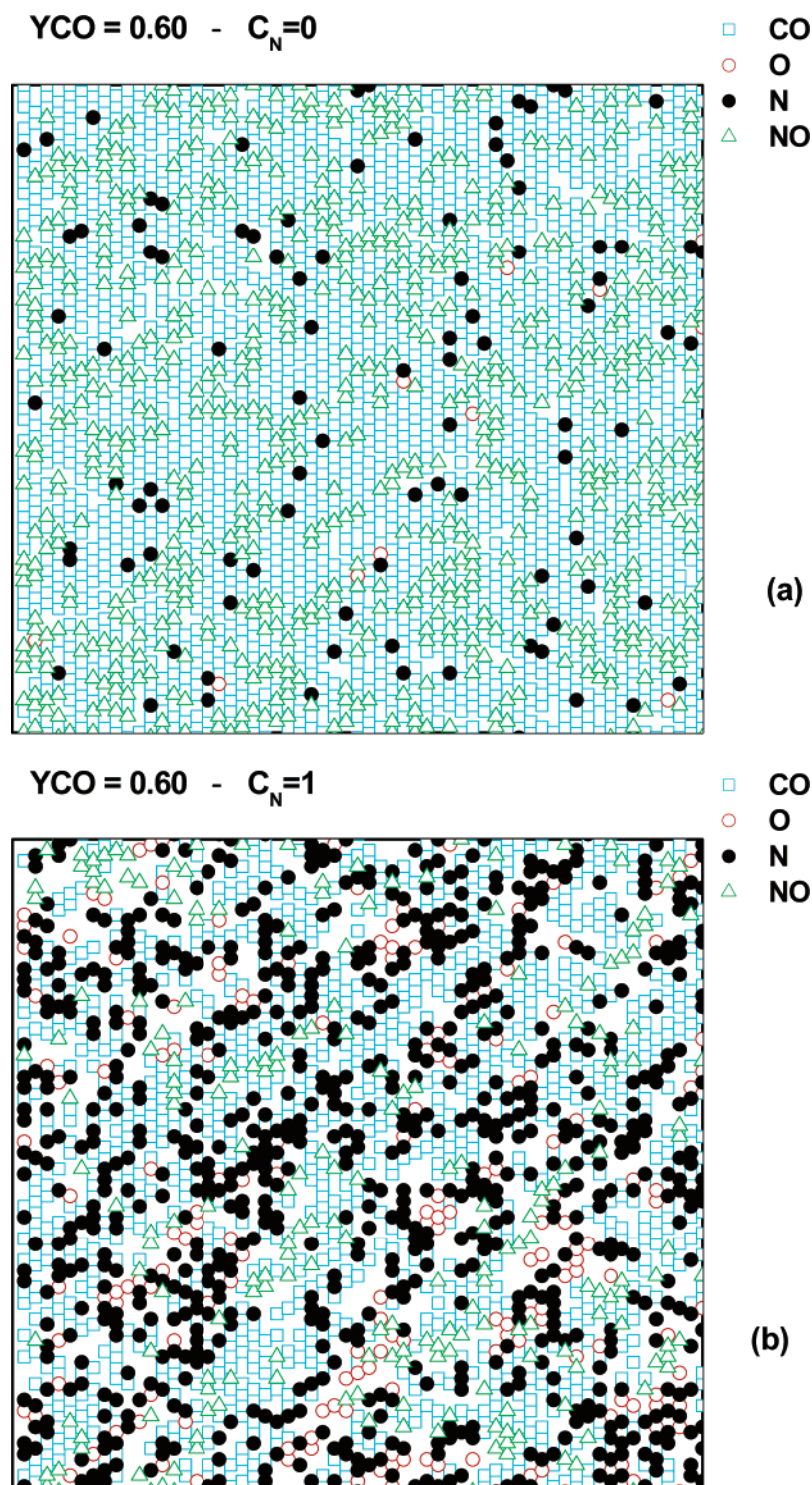


Figure 4. Snapshots of the surface adsorbed species during the Monte Carlo simulation at $Y_{\text{CO}} = 0.6$, showing the effect of the formation of N islands: (a) $C_{\text{N}} = 0$, corresponding to no island formation; (b) $C_{\text{N}} = 1$, where island formation is allowed to occur.

of the coverage of the adsorbed species is also similar (except that the O and N coverages are about double than before). It can therefore be concluded that the $\text{N} + \text{N}$ pathway plays only a minor role in influencing the overall results obtained with our model. This may have been to some extent expected because of the way the values of the kinetic parameters were chosen (see above), but it is in contrast with our previous study where all elementary reaction steps were considered as instantaneous, in which case more drastic effects were observed.³³

A clear difference is also seen in the data in Figure 2, right side, which reports results for the case where the pathway

involving the $(\text{N}-\text{NO})^*$ intermediate (steps 4 and 5) is turned off instead, leaving the N recombination step as the only one to produce N_2 . There, quite noticeable modifications in the behavior of the system are observed, more marked than those observed in the previous simulations.³³ In particular, the surface oxygen atoms reach unreasonably high coverages at low Y_{CO} values, the N coverage is also too high at low and intermediate Y_{CO} values, and the production rates of N_2 and CO_2 are depressed over the whole range of molar fractions. All those predictions, especially the high O coverage at low Y_{CO} , sharply contradict the experimental observations. The main conclusion

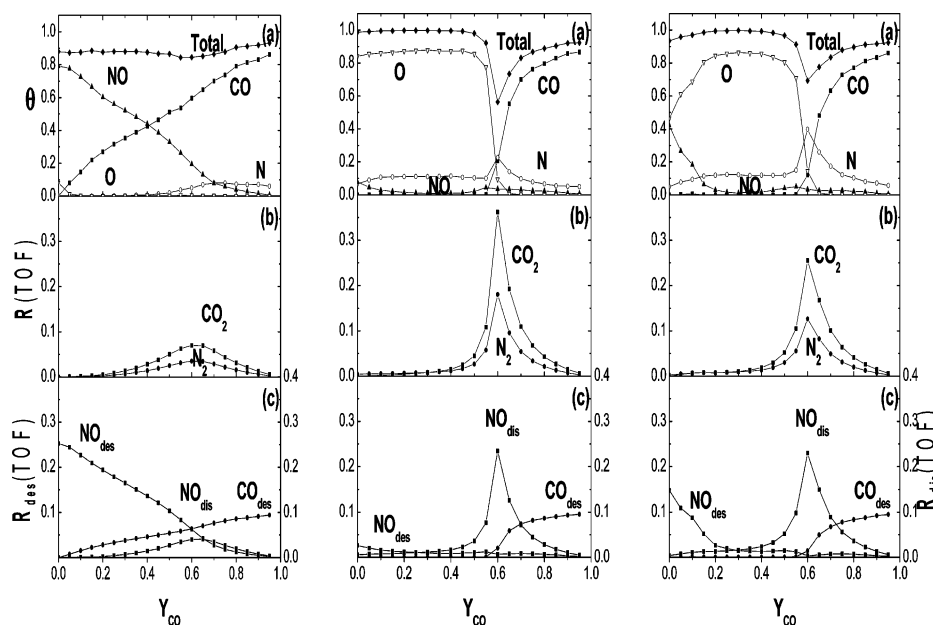


Figure 5. Left: effect of neglecting the surface diffusion of NO and CO. Middle: effect of neglecting the blockage of NO dissociation by neighboring coadsorbed NO species, which was simulated by setting $C_{NO} = 0$. Right: effect of neglecting the $(N-NO)^*$ formation rate enhancement due to neighboring coadsorbed NO species, as obtained by setting $C_{N-NO} = 0$. The remaining parameters were kept the same as in Figure 1.

from these data is that the $(N-NO)^*$ intermediary pathway is of fundamental importance for the NO + CO reaction.

The effect of N-island formation was then tested by making $C_N = 0$ in eq 17. From the results shown in Figure 3, it can be seen that the consequences of neglecting the formation of these islands are important only in the sense that the rates of production of N_2 and CO_2 are both slightly depressed, as also are the N and O coverages. This can be due to the fact that N atoms are always rapidly removed from the surface through steps 4, 5, and 6, and that, when N islands are allowed to form, they never reach large sizes. This is explicitly shown by the snapshots of the surface composition taken during the Monte Carlo simulation at $Y_{CO} = 0.6$ and presented in Figure 4. Clearly, no nitrogen islands are seen with $C_N = 0$. On the other hand, some islands do form with $C_N = 1$ (Figure 4b), but they are still quite small, averaging 2–8 atoms per island, and typically display highly irregular shapes.

In a similar way, it was shown that neglecting either CO or NO diffusion (or both) also causes similar perturbations to the kinetics of the system: again, only a depression in the production rates is seen in Figure 5, left side. This means that the CO and NO adsorption–desorption processes somehow compensate for the lack of surface diffusion. Similar results were reported before.³³ The central part of the figure shows the results of neglecting the site-blocking effect on the dissociation of NO due to the presence of other coadsorbed NO species, which was shut off by making $C_{NO} = 0$. The lifting of such a restriction leads to enhanced production rates, but, unfortunately, also to a very high O coverage at low CO gas-phase concentrations. This, as already mentioned, is in contradiction with experimental results. Since no other way could be visualized to limit the accumulation of atomic O at low Y_{CO} , it is concluded that the site-blocking effect, as suggested by experiments,³⁴ is also of fundamental importance to the NO reduction mechanism. Finally, the effect of enhancing the probability of formation of the $(N-NO)^*$ intermediate via the presence of coadsorbed NO species was probed. In contrast to the results from our latest reported simulations,³³ it was found here that when this effect is neglected by making $C_{N-NO} = 0$, a very high O coverage at low Y_{CO} is again obtained (right side of the figure).

It is worth highlighting the self-consistency of the three sets of results shown in Figures 2 (right) and 5 (middle and right). In all of them the reaction pathway involving the formation of the $(N-NO)^*$ intermediate is eliminated or depressed: while in Figure 2 (right) it is eliminated directly, in Figure 5 (middle) it is depressed by the elimination of the blocking effect on NO dissociation, which depresses the existence of undissociated NO, and in Figure 5 (right) by the elimination of the enhancing effect of coadsorbed NO species on the formation of the intermediate. Consequently, the same unwanted high O coverages at low Y_{CO} is obtained in all three cases. In summary, the present study strongly supports the reaction scheme suggested by the experiments^{8,19,21,25,48} where the production of N_2 takes place mainly through the formation of a $(N-NO)^*$ intermediate.

Once the relative importance of the different elementary steps to the overall NO reduction kinetics was determined, our next step was to test the usefulness of our model in determining the variations in reaction rates with temperature and gas-phase compositions against those measured experimentally.⁸ This was done by fixing the parameter values to those used in Figure 1. Figure 6 shows a comparison of the experimental versus simulation results for the variation of the reaction rate with temperature for four NO:CO ratios in the gas mixture. The agreement is quite satisfactory, especially regarding the position of the maximum in reaction rate as a function of temperature and beam composition. It was also made sure that the simulations in all cases yielded almost identical results for R_{CO_2} and $2 \times R_{N_2}$, as should be the case according to stoichiometric arguments, and as has been seen experimentally.⁸ There are slight differences in the quantitative values for the reaction rates in Figure 6 between the experiments and the simulations, of about a factor of 2, but these are not particularly significant because those rates are quite sensitive to the initial sticking coefficients and absolute molecular fluxes used in the simulations. In fact, the NO and CO initial sticking coefficients vary in a quite complex way with temperature and gas composition, fluctuating between 0.05 and 0.7.²⁰ As indicated in Table 1, in order to simplify the calculations, here we used unique values for S_0 (0.3 for NO and 0.2 for CO) for all temperatures and gas-phase compositions; the use of lower S_0 values would be

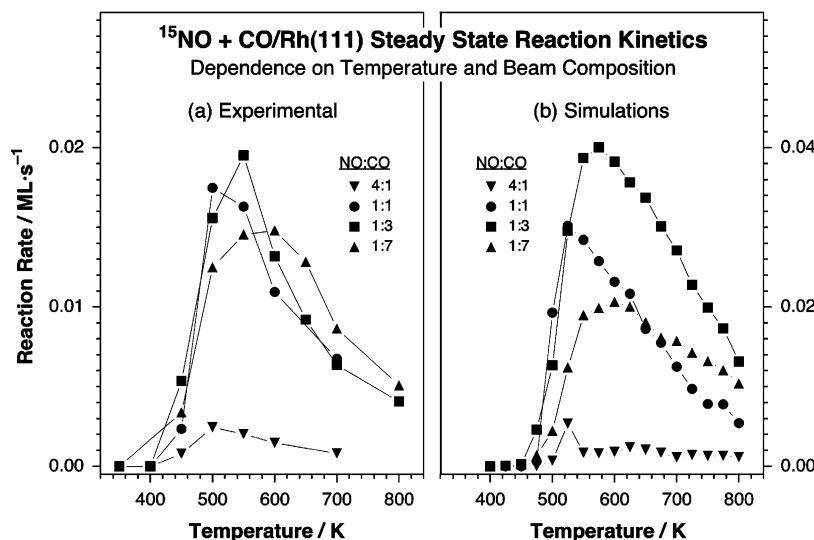


Figure 6. Variations in reaction rates with temperature for different NO:CO gas compositions. Left: experimental data.⁸ Right: results from our Monte Carlo simulations.

expected to reduce the overall reaction rates estimated with our model. In general, it is concluded that the kinetic model presented here is able to correctly predict the most important aspects of the behavior of the NO + CO/Rh(111) system, in particular the variations in N₂ production rate as a function of temperature and NO and CO composition in the gas phase.

4. Conclusions

In this work our previous model³³ for the description of the kinetics of NO reduction by CO on Rh(111) single-crystal surfaces was extended to incorporate temperature-dependent reaction rates for all the elementary processes involved. This resulted in a more realistic description of the system, with predictions showing some differences with those reported before.³³ Of particular importance is the fact that the new model was capable of testing absolute values for the reaction rates and suitable to follow the reaction kinetics as a function of temperature. With that, the model explained the following recent experimental observations:

(a) the production of N₂ through the formation and subsequent decay of a (N–NO)* intermediate species (in addition to the classical N + N recombination step) and the facilitation of this process by the presence of neighboring coadsorbed NO molecules;

(b) the formation of N islands; and

(c) the depression of the NO dissociation probability by the presence of neighboring coadsorbed NO species.

In addition, the new model also incorporated other elementary processes, such as desorption and surface diffusion of NO and CO. The overall behavior of the reaction in steady state, obtained by dynamic Monte Carlo simulations with temperature-dependent transition rates for all elementary processes involved, was found to be in good agreement with experimental observations. The relative contribution of the kinetics of each individual elementary step to the overall reaction rate was estimated by turning them off selectively in the simulations.

Overall, the present study supports a reaction scheme where the production of N₂ is assumed to result mainly from a pathway involving the formation of a (N–NO)* intermediate and defines a reliable model capable for predicting the changes in reaction rates as a function of temperature and NO:CO gas composition.

Further progress in the subject could be achieved by combining first-principles density functional theory calculations of

the energetics of the relevant elementary processes with dynamic Monte Carlo simulations, in a similar way as done, for example, by Scheffler et al.⁴⁹ for CO oxidation.

Acknowledgment. The present work was partially supported by CONICET (Argentina) and CONACyT (México) through a bilateral cooperation program. Additional funding was provided by the U.S. National Science Foundation.

References and Notes

- Belton, D. N.; Taylor, K. C. *Curr. Opin. Solid State Mater. Sci.* **1999**, *4*, 97.
- Shelef, M.; McCabe, R. W. *Catal. Today* **2000**, *62*, 35.
- Heck, R. M.; Farrauto, R. J. *Appl. Catal. A* **2001**, *221*, 443.
- Shelef, M.; Graham, G. W. *Catal. Rev.-Sci. Eng.* **1994**, *36*, 433.
- Oh, S. H.; Fisher, G. B.; Carpenter, J. E.; Goodman, D. W. *J. Catal.* **1986**, *100*, 360.
- Belton, D. N.; Schmieg, S. J. *J. Catal.* **1993**, *144*, 9.
- Bowker, M.; Guo, Q.; Li, Y.; Joyner, R. W. *J. Chem. Soc., Faraday Trans.* **1995**, *91*, 3663.
- Gopinath, C. S.; Zaera, F. *J. Catal.* **1999**, *186*, 387.
- Hopstaken, M. J. P.; van Gennip, W. J. H.; Niemantsverdriet, J. W. *Surf. Sci.* **1999**, *435*, 69.
- Zaera, F.; Gopinath, C. S. *J. Mol. Catal. A* **2001**, *167*, 23.
- Requejo, F. G.; Hebenstreit, E. L. D.; Ogletree, D. F.; Salmeron, M. *J. Catal.* **2004**, *226*, 83.
- Zaera, F. Surface science studies of the mechanism of NOx conversion: Correlations between kinetics in vacuum and under catalytic conditions. In *Past and Present in DeNOx Catalysis: From Molecular Modeling to Chemical Engineering*; Granger, P., Parvulescu, V., Eds.; Elsevier: Amsterdam, In press.
- Yaldram, K.; Khan, M. A. *J. Catal.* **1991**, *131*, 369.
- Albano, E. V. *Heter. Chem. Rev.* **1996**, *3*, 389.
- Zhdanov, V. P.; Kasemo, B. *Surf. Sci. Rep.* **1997**, *29*, 31.
- Cortés, J.; Puschmann, H.; Valencia, E. *J. Chem. Phys.* **1998**, *109*, 6086.
- Dickman, A. G.; Grandi, B. C. S.; Figueiredo, W.; Dickman, R. *Phys. Rev. E* **1999**, *59*, 6361.
- Bustos, V. A.; Zgrablich, G. *Int. J. Mod. Phys. C* **1999**, *10*, 1077.
- Zaera, F.; Gopinath, C. S. *J. Chem. Phys.* **1999**, *111*, 8088.
- Gopinath, C. S.; Zaera, F. *J. Phys. Chem. B* **2000**, *104*, 3194.
- Zaera, F.; Gopinath, C. S. *Chem. Phys. Lett.* **2000**, *332*, 209.
- Zaera, F.; Wehner, S.; Gopinath, C. S.; Sales, J. L.; Gargiulo, V.; Zgrablich, G. *J. Phys. Chem. B* **2001**, *105*, 7771.
- Gopinath, C. S.; Zaera, F. *J. Catal.* **2001**, *200*, 270.
- Zaera, F.; Gopinath, C. S. *J. Chem. Phys.* **2002**, *116*, 1128.
- Zaera, F.; Gopinath, C. S. *Phys. Chem. Chem. Phys.* **2003**, *5*, 646.
- Wehner, S.; Paffett, M. T.; Zaera, F. *J. Phys. Chem. B* **2004**, *108*, 18683.
- Meng, B.; Weinberg, W. H.; Evans, J. W. *J. Chem. Phys.* **1994**, *101*, 3234.

- (28) Khan, M. A.; Yaldram, K.; Khalil, G. K.; Khan, K. M. *Phys. Rev. E* **1994**, *50*, 2156.
- (29) Williams, F. J.; Aldao, C. M.; Palermo, A.; Lambert, R. M. *Surf. Sci.* **1998**, *412–413*, 174.
- (30) Bustos, V.; Gopinath, C. S.; Uñac, R.; Zaera, F.; Zgrablich, G. *J. Chem. Phys.* **2001**, *114*, 10927.
- (31) Zhdanov, V. P.; Kasemo, B. *Surf. Sci.* **2002**, *496*, 251.
- (32) Bustos, V.; Uñac, R.; Zaera, F.; Zgrablich, G. *J. Chem. Phys.* **2003**, *118*, 9372.
- (33) Avalos, L. A.; Bustos, V.; Uñac, R.; Zaera, F.; Zgrablich, G. *J. Mol. Catal. A* **2005**, *228*, 89.
- (34) Borg, H. J.; Reijerse, J. F. C.-J. M.; van Santen, R. A.; Niemantsverdriet, J. W. *J. Chem. Phys.* **1994**, *101*, 10052.
- (35) Yates, J. T., Jr.; Goodman, D. W. *J. Chem. Phys.* **1980**, *73*, 5371.
- (36) Barteau, M. A.; Ko, E. I.; Madix, R. J. *Surf. Sci.* **1981**, *102*, 99.
- (37) Behm, R. J.; Thiel, P. A.; Norton, P. R.; Ertl, G. *J. Chem. Phys.* **1983**, *78*, 7437.
- (38) Yeo, Y. Y.; Vattuone, L.; King, D. A. *J. Chem. Phys.* **1996**, *104*, 3810.
- (39) Xu, M.; Liu, J.; Zaera, F. *J. Chem. Phys.* **1996**, *104*, 8825.
- (40) Thiel, P. A.; Yates, J. T., Jr.; Weinberg, W. H. *Surf. Sci.* **1979**, *82*, 22.
- (41) Castner, D. G.; Somorjai, G. A. *Appl. Surf. Sci.* **1980**, *6*, 29.
- (42) Peterlinz, K. A.; Sibener, S. J. *J. Phys. Chem.* **1995**, *99*, 2817.
- (43) Xu, H.; Ng, K. Y. S. *Surf. Sci.* **1996**, *365*, 779.
- (44) Berko, A.; Solymosi, F. *Appl. Surf. Sci.* **1992**, *55*, 193.
- (45) Hinrichsen, H. *Adv. Phys.* **2000**, *49*, 815.
- (46) van Kampen, N. G. *Stochastic Processes in Physics and Chemistry*; North-Holland: Amsterdam, 1992.
- (47) Hopstaken, M. J. P.; Niemantsverdriet, J. W. *J. Chem. Phys.* **2000**, *113*, 5457.
- (48) Aryafar, M.; Zaera, F. *J. Catal.* **1998**, *175*, 316.
- (49) Reuter, K.; Scheffler, M. *Phys. Rev. B* **2006**, *73*, 045433.